crystals

MDPI

Article

Structural Study of *N*-(1,3-Benzothiazol-2-yl)-4-Halobenzenesulfonylhydrazides: Hirshfeld Surface Analysis and PIXEL Calculations

Ligia R. Gomes [1,2,3,*], John N. Low [4], Alessandra C. Pinheiro [5] and James L. Wardell [4,5,*]

1 LaQV, REQUIMTE, Faculdade de Ciências, Universidade do Porto, Rua do Campo Alegre, 687, 4169-007 Porto, Portugal
2 Escola Superior de Saúde da UFP, Universidade Fernando Pessoa, Rua Carlos da Maia, 296, 4200-150 Porto, Portugal
3 FP-I3ID, Universidade Fernando Pessoa, Praça 9 de Abril, 349, 4249-004 Porto, Portugal
4 Department of Chemistry, University of Aberdeen, Old Aberdeen AB24 3UE, Scotland, UK; j.n.low@abdn.ac.uk
5 Fiocruz–Fundação Oswaldo Cruz, Instituto de Tecnologia em Farmacos—Farmanguinhos, Sizenando Nabuco 100, Manguinhos 21041-250, RJ, Brazil
* Correspondence: lrgomes@ufp.edu.pt (L.R.G.); che415@abdn.ac.uk (J.L.W.)

Abstract: Hydrazonylsulfones such as Bt-NHNHSO$_2$R and their iminotautomers have been studied as optical materials and for their biological potential. In this work, a structural study has been carried out on *N*-(1,3-benzothiazol-2-yl)-4-(halogenobenzenesulfonyl)-hydrazides (**1**: X = F, Cl, Br). For (**1**: X = F), single-crystal X-ray diffraction, Hirshfeld surface analysis, and PIXEL calculations were conducted, while in (**1**: X = Cl) and (**1**: X = Br), only single-crystal X-ray diffraction studies were successfully conducted due to the disordering of the solvent. Each compound crystallises with two independent but similar amino tautomers in the asymmetric units: compound (**1**: X = F) crystallises in the monoclinic P21/c, and the isostructural pair (X: **1** = Cl and Br) crystallises in the tetragonal P-421c space group. In the most stable motif of the supramolecular arrangement, the molecules of the asymmetric unit are connected by classical N–H(hydrazinyl)···N(thiazoyl) hydrogen bonds and several face-to-face, offset π···π interactions. This motif has a very powerful influence on the crystal structure due to its direct links with the other weaker motifs. Other significant intermolecular interactions found in the structure include N–H(hydrazonyl)···O(sulfonate) bonds. Analogous intermolecular interactions were found in similar compounds, leading to the conclusion that those interactions are the most important instabilizing the solid state of hydrazonylsulfones.

Keywords: hydrazonylsulfones; 1,3-benzothiazol; X-ray; PIXEL calculations; lattice energies

Citation: Gomes, L.R.; Low, J.N.; Pinheiro, A.C.; Wardell, J.L. Structural Study of *N*-(1,3-Benzothiazol-2-yl)-4-Halobenzenesulfonylhydrazides: Hirshfeld Surface Analysis and PIXEL Calculations. *Crystals* **2024**, *14*, 330. https://doi.org/10.3390/cryst14040330

Academic Editor: Emilio Parisini

Received: 5 March 2024
Revised: 14 March 2024
Accepted: 26 March 2024
Published: 30 March 2024

1. Introduction

The 1,3-benzothiazolyl framework is a constituent of several compounds that have been studied in a range of different areas, with focuses on their pharmacological activities [1–9], their applications in optical materials [10,11], their functions in liquid crystals [12], and their potential uses as agents in industrial processes [13]. Although these types of compounds exist naturally, they are rare [14]. Thus, several synthetic methodologies have been developed over the years in order to obtain them. Of particular interest are the 2-hydrazinyl-1,3-benzothiazole derivatives Bt-NHNH$_2$, **I**, which can be found also in their imino form, **IA** (R = H or alkyl; see Figure 1), and have been studied both in their own right and as precursors of other related compounds [15–17] such as the hydrazones, Bt-NHN=CHR$_1$, **II**, and their imino analogues, **IIA** [18–20]. A special group of derivatives are the hydrazonylsulfones, such as Bt-NHNHSO$_2$R, **III**, and their iminotautomers, **IIIA** (see Figure 1).They played a significant part in the work of Huenig and co-workers in the late 1950s to early 1970s [21,22] and in several patents submitted by Agfa, essentially because of

their optical properties [23]. Over subsequent years, patents and articles have reported on an expanded range of potential applications, namely as ligands for metal extraction [24] and as optical materials [25], as well as for their possible biological uses, for example as fibroblast growth factor antagonists [26], as autotaxin inhibitors [27] and as inhibitors of Wnt antagonist DKK [28] and cytosolic phospholipase A2α [29].

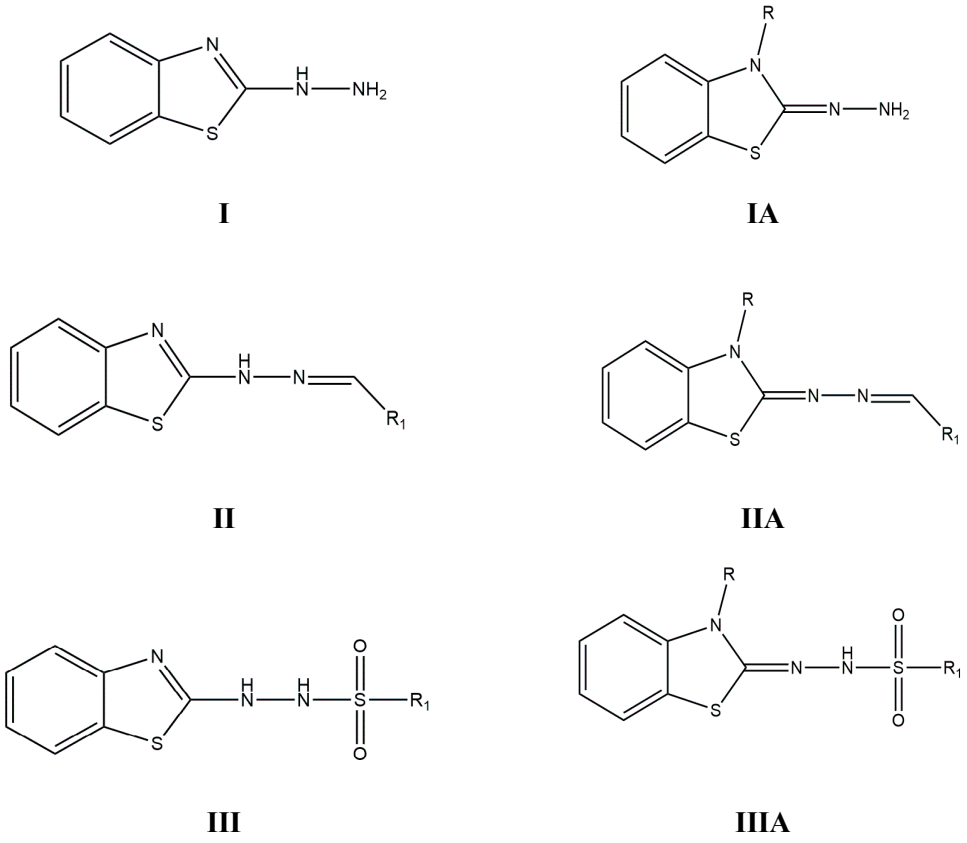

Figure 1. Chemical structures of selected benzothiazolyl derivatives.

Substituted [N-(1,3-benzothiazol-2-yl)nitrobenzenesulfonyl-hydrazides], Bt-NHNHS-$(O)_2C_6H_4X$ family of compounds, have been previously obtained by Peretyazhko et al. [30] using an elaborate synthetic route that consisted of the oxidative cyclization of substituted 1,4-diphenylthiosemicarbazides with potassium ferricyanide in alkaline alcoholic media, but we recently managed to obtain some of those compounds, e.g., Bt-NHNHS$(O)_2C_6H_4X$, (**1**: X = H) [31] (**1**: X = 2, 3-, 4-O_2N) [32], Scheme 1, by direct reaction between Bt-$NHNH_2$ and $XC_6H_4SO_2Cl$, albeit with variable yields. However, when we attempted the corresponding reaction with 4-$IC_6H_4SO_2Cl$, we obtained the product Bt-N(C_6H_4-I-4)NH_2 [33]. The regiochemistry of this last reaction remains unknown, but we hypothesized that a specific iodo-heteroarene interaction that occurred prior to the reaction between Bt-$NHNH_2$ and 4-$IC_6H_4SO_2Cl$ arranged the reactants to facilitate a reaction involving the non-terminal nitrogen. When Bt-$NHNH_2$ reacts with $XC_6H_4SO_2Cl$, only the amino tautomers are formed. Furthermore, only a single regioisiomer was obtained in each of the syntheses. The synthesis of 3-alkylated imine derivatives **IIIA** almost invariably involves the reaction of the sulfonyl chloride with a preformed imino precursor [34].

We now wish to report further on reactions between arenesulfonyl chlorides and Bt-$NHNH_2$ and to report on a structural study of three halo derivatives, 4-F-, 4-Cl- and 4-Br-C_6H_4NHNH-Bt (**1**: X = F, Cl and Br, respectively), see Scheme 1.

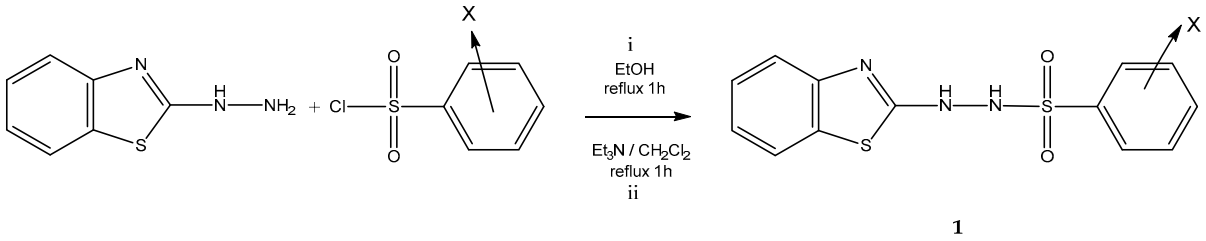

1: X=H

1: X= 2-,3-,4-O_2N

1: X= 4-F, 4-Cl, 4-Br

Scheme 1. Chemical reactions used to obtain the compounds **1**: X = H [31]; **1**: X = 2-,3-,4-O_2N [32].

2. Materials and Methods

2.1. Instruments

Melting points were determined on a Buchi (B-545) instrument and are presented uncorrected. IR spectra were obtained using a Nicolet 6700 FTIR instrument (Waters Corporation, Milford, MA, USA) by ATR (Attenuated Total Reflectance, Blagnac, France). NMR spectra were recorded on Bruker Avance 400 and500 spectrometers (Billerica, MA, USA) in DMSO-d_6 solution at room temperature. Accurate mass measurements were determined using a Water Mass Spectrometer Model Xevo G2 QT instrument (Waters Corporation, Milford, MA, USA).

2.2. General Synthesis

Two synthesis reactions were employed (see Scheme 1).

(i) A solution of 2-hydrazinyl-1,3-benzothiazole(1 mmol) and the arenesulfonyl chloride (1 mmol) in EtOH (20 mL) was refluxed for 1 h. The reaction mixture was washed with water, then the organic layer was collected, dried over magnesium sulphate, and rotary evaporated. The residue was recrystallized from an ethanol solution.

(ii) To a stirred solution of 2-hydrazinobenzothiazole (1 mmol) in dichloromethane (12 mL) were sequentially added 2 drops of Et3N and the appropriate arenesulfonyl chloride (1.20 mmol). The reaction mixture was stirred for 24 h at room temperature and concentrated under reduced pressure. The residue was purified by column chromatography using dichloromethane/methanol (100→95%) as an eluent, resulting inthe benzothiazolyl derivatives in 40–65% yields.

2.2.1. 2-[2-(4-Fluorobenzenesulfonyl)Hydrazinyl]-1,3-Benzothiazol, (**1**: X = F)

Prepared using method (ii) from 2-hydrazinyl-1,3-benzothiazole and 4-fluorobenzenesulfonyl chloride. m.p. 110–112 °C; yield 60%.

^{1}H NMR (500 MHz, DMSO-d_6). δ (ppm): 9.40 (1H, *s*, NH), 8.20 (2H, *m*, H2′ & H6′), 7.88 (1H, *dd*, *J* = 7.9 & 1.2, H4), 7.64 (1H, *dd*, *J* = 8.2 & 1.1, H7), 7.48 (2H, *m*, H3′ & H5′), 7.37 (1H, *ddd*, *J* = 8.2, 7.3 & 1.2, H6); 7.24 (1H, *ddd*, *J* = 7.9, 7.3 & 1.1, H5), 5.76 (1H, *s*, NH).

^{13}C NMR (125 MHz, DMSO-d_6): δ: 166.2; 165.2; 156.0; 132.9; 132.0; 132.0; 131.9; 126.0; 123.4; 121.4; 120.7; 116.2; 116.1 ppm.

IR (cm^{-1}, KBr): 3330 (N-H); 3060 (Ar-H), 1351 & 1153 (SO_2), 1040 (C-F)

HR-MS (ESI): Calcd for $C_{13}H_{10}FN_3NaO_2S_2^+$ (M^+ Na^+): 246.0091; Found: 246.0086.

2.2.2. 2-[2-(4-Chlorobenzenesulfonyl)Hydrazinyl]-1,3-Benzothiazol, (**1**: X = Cl)

Prepared via method (i) from 2-hydrazinyl-1,3-benzothiazole and 4-chlorobenzenesulfonyl chloride. m.p. 172–174 °C; yield 61%.

^{1}H NMR (400 MHz, DMSO-d_6). δ (ppm): 9.40 (1H, *s*, NH), 8.14 (2H, *d*, phenyl), 7.90 (1H, *d*, H4), 7.72 (2H, *d*, phenyl), 7.64 (1H, *dd*, H7), 7.37 (1H, *m*, H6), 7.26 (1H, *m*, H5), 5.59 (*s*, 1H).

^{13}C NMR (100 MHz, DMSO-d_6): δ 165.2, 150.9, 139.2, 135.4, 132.1, 130.6, 129.1., 127.6, 127.4, 126.0, 123.4, 121.5, 120.7 ppm.

IR (cm^{-1}, KBr): 3330 (N-H); 3090 (Ar-H), 1366 & 1164 (SO_2).

HR-MS (ESI): Calcd for $C_{13}H_{10}ClN_3NaO_2S_2^+$ (M^+ Na^+): 361.9795; Found: 361.9812.

2.2.3. 2-[2-(4-Bromobenzenesulfonyl)Hydrazinyl]-1,3-Benzothiazol (**1**: X = Br)

Prepared via method (i) from 2-hydrazinyl-1,3-benzothiazole and 4-bromobenzenesulfonyl chloride. m.p. 172–174 °C; yield 61%.

^{1}H NMR (400 MHz, DMSO-d_6). δ (ppm): 8.10 (*d*, 2H), 7.88 (1H, *dd*, H), 7.72 (*d*, 2H), 7.64 (1H, *dd*, H7), 7.33 (1H, *m*, H6), 7.28 (1H, *m*, H5), 5.75 (*s*, 1H).

IR (cm^{-1}, KBr): 3330 (N-H); 3090 (Ar-H), 1371 & 1154 (SO_2).

HR-MS (ESI): Calcd for $C_{13}H_{10}BrN_3NaO_2S_2^+$ (M^+ Na^+): 361.9795; Found: 361.9802.

2.3. X-ray Data Collection and Structure Refinement

All details on data collection, structure determination, and refinement are listed in Table S1 (Supplementary Materials). The computer programs used were CrystalClear-SM Expert 3.1 b27 and CrysAlis PRO 1.171.42.51a [35], OSCAIL V6 [36], SHELXT [37], ShelXle [38] SHELXL2018/1 [39], PLATON [40], and Mercury [41]. Compounds **1**: X = Br and **1**: X = Cl exhibited disordered solvent molecules, and SQUEEZE was applied as implemented in PLATON. The procedure accounts for the contribution of a (heavily) disordered solvent to the calculated structure factors by back-Fourier transformation of the continuous density found in a masked region of the difference map. For **1**: X = Cl, the solvent accessible volume was 579 Å, with 155 electrons found; for **1**: X = Br, the solvent accessible volume was 568 Å, with 172 electrons found. The positions of the actual solvent molecules could not be resolved.

2.4. Lattice Energy and Intermolecular Interaction Energy Calculations

Lattice energies and intermolecular interaction energies were calculated using PIXEL code implemented in the CLP package [42,43]. The intermolecular energies were assigned by distributed charge description after a preliminary evaluation of charge density from GAUSSIAN at the MP2/6-311G** level of theory (CUBE option).

2.5. Hirshfeld Surface Analysis and Two-Dimensional Fingerprint (FP) Plots

The Hirshfeld surfaces and two-dimensional fingerprint (FP) plots [44] were generated using Crystal Explorer 3.1 [45]. The Hirshfeld surfaces were mapped over d_{norm} and over electrostatic potential (ESP),which was calculated using Becke88 [46] and LYP [47] for correlation and exchange potential at the 6-311G(d,p) level, as implemented in Crystal Explorer 3.1 [45]. The 2D FP plots were derived from the HS analysis.

3. Results

3.1. Molecular Structures

The samples used to determine the X-ray structures were grown from dilute ethanol solutions at room temperature. Compound (**1**: X = F) crystallizes in the monoclinic space group P21/c, with Z = 8, while the isostructural compounds, (**1**: X = Cl and Br), crystallize in the tetragonal space P-42_1c group with Z = 16. Two similar independent molecules, Mol 1 and Mol 2, comprise the asymmetric units of each of (**1**: X = F, Cl and Br). The molecular structures with the atom-numbering schemes of the two independent molecules for compounds **(1**: X = F, Cl and Br) are shown in Figure 2; similar numbering schemes have been used for the three compounds. Selected bond lengths, geometric parameters for intramolecular H bonds, and selected dihedral angles are given in Tables 1–3.

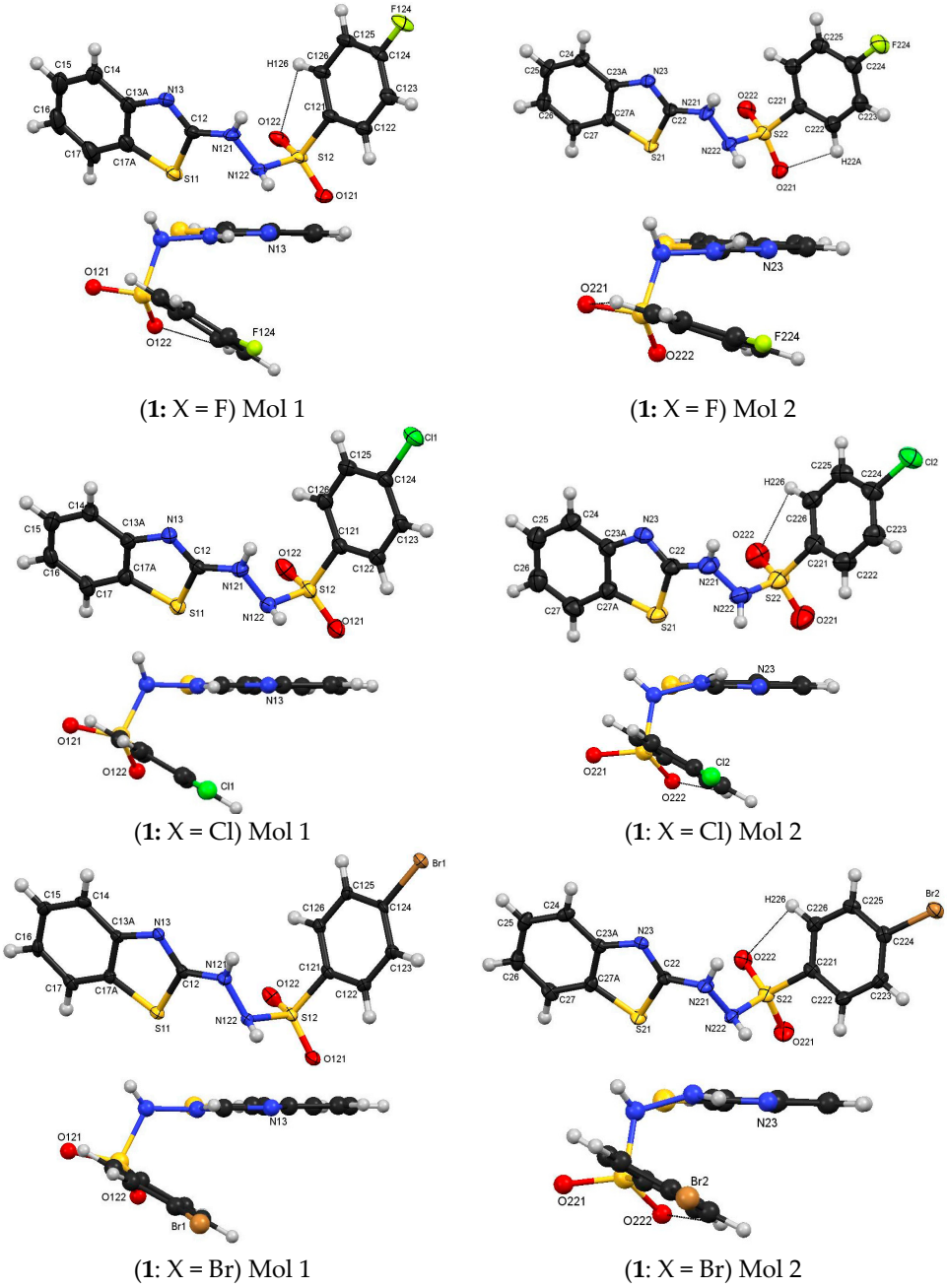

Figure 2. Atom arrangements, numbering schemes and 'U' and 'J' molecular shapes for structures of (**1**: X = F, Cl and Br).

Table 1. Selected bond lengths Å [1].

Compound	Cn2-Nn21	Nn21-Nn22	Nn22-Sn2	Sn2-Cn21
(**1**: X = F)				
Mol A: n = 1	1.351(3)	1.393(2)	1.6565(17)	1.7555(19)
Mol B: n = 2	1.343(3)	1.391(3)	1.6691(18)	1.750(2)
(**1**: X = Cl)				
Mol A: n = 1	1.350(5)	1.401(4)	1.659(3)	1.749(3)
Mol B: n = 2	1.364(6)	1.396(4)	1.645(4)	1.757(2)
(**1**: X = Br)				
Mol A: n = 1	1.358(7)	1.396(6)	1.663(4)	1.756(5)
Mol B: n = 2	1.356(7)	1.405(7)	1.647(5)	1.776(5)

[1] Standard bond lengths: C-N = 1.45, C=N = 1.27; N-N = 1.41; N=N = 1.27 Å.

Table 2. Intramolecular hydrogen bonds (Å, °).

Compound	D–H···A	D–H	H···A	D···A	D–H···A
(**1**: X = F)	C222–H22A···O221	0.95	2.52	2.900(3)	104
(**1**: X = F)	C126–H126···O122	0.95	2.60	2.945(2)	102
(**1**: X = Cl)	C226–H226···O222	0.95	2.56	2.922(6)	103
(**1**: X = Br)	C226–H226···O222	0.95	2.56	2.922(6)	103

Table 3. Dihedral angles (°).

Compound	Angle between Bt & Ph Planes	Angle between SO_2 and	
	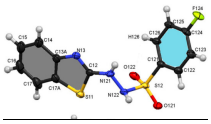	Ph	Bt
(**1**: X = F)			
Mol 1	30.93 (8)	40.82	48.36
Mol 2	16.64 (9)	48.96	47.66
(**1**: X = Cl)			
Mol 1	30.53 (16)	42.31	46.35
Mol 2	29.21 (18)	50.24	55.26
(**1**: X = Br)			
Mol 1	29.7 (2)	41.64	46.67
Mol 2	28.3 (2)	51.46	56.34

3.2. Intermolecular Interactions

Relevant intermolecular interactions found by PLATON [39] are listed in Supplementary Tables S2–S4. Table 4 shows the classic hydrogen bonds, Table 5 the Y–X···π interactions, and Table 6 the geometric parameters related to the π···π interactions.

Table 4. Geometric parameters (Å, °), for the intermolecular hydrogen bonds.

Cpd	D–H···A	D–H	H····A	D···A	D–H···A	Symmetry Code
1: X = 4-F	N121–H121···N23	0.78(3)	2.08(3)	2.835(2)	165(3)	x, y, z
	N221–H221···N13	0.86(3)	1.94(3)	2.775(2)	165(3)	x, y, z
	N122–H122···O122	0.85(3)	2.15(3)	2.989(2)	168(2)	$x, 1/2 - y, 1/2 + z$
	N222–H222···O221	0.99(2)	1.88(2)	2.862(3)	177(2)	$-x, 1 - y, 1 - z$
	C16–H16···O121	0.95	2.44	3.360(3)	162	$-1 + x, 1/2 - y, -1/2 + z$
	C24–H24···O121	0.95	2.55	3.315(3)	138	$x, 1/2 - y, 1/2 + z$
	C25–H25···O122	0.95	2.62	3.232(3)	123	$x, y, 1 + z$
1: X = 4-Cl	N121–H121···N23	0.88	2.00	2.861(5)	166	x, y, z
	N122–H122···O122	0.97	2.11	2.971(4)	147	$1/2 - y, 1/2 - x, -1/2 + z$
	N221–H221···N13	0.88	2.07	2.855(5)	149	x, y, z
	C26–H26···Cl1	0.95	2.81	3.649(5)	148	$-1/2 + y, 1/2 + x, -1/2 + z$
1: X = 4-Br	N121–H121···N23	0.88	2.00	2.864(6)	166	x, y, z
	N122–H122···O122	0.88	2.37	2.979(6)	127	$3/2 - y, 3/2 - x, 1/2 + z$
	N221–H221···N13	0.88	2.10	2.868(6)	145	x, y, z

Table 5. Geometric parameters (Å, °) for the Y–X···π interactions *.

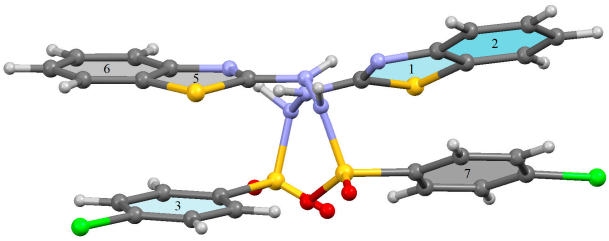

Cpd	Y–X···π	X···Cg(π)	X_{perp}	Y–X···Cg(π)	Y···Cg(π)	Symmetry Code
1: X = 4-F	C17–H17···Cg1	2.84	2.77	132	3.542(3)	$x, 1/2 - y, -1/2 + z$
	C124–F124···Cg6	3.7122(16)	3.684	76.07(10)	3.632(3)	x, y, z
	C224–F224···Cg2	3.853(2)	3.622	71.24(13)	3.542(3)	x, y, z
1: X = 4-Cl	C17–H17···Cg1	2.83	2.72	131	3.526(4)	$1/2 - y, 1/2 - x, 1/2 + z$
	C124–Cl1···Cg6	3.718(2)	3.471	131	3.632(3)	x, y, z
1: X = 4-Br	C17–H17···Cg1	2.79	2.72	135	3.526(4)	$1/2 - x, 1/2 - y, 1/2 + z$
	C124–Br1···Cg6	3.824(2)	3.556	66.37(16)	3.522(6)	x, y, z

* See figure in the table for number of the Cg's.

Table 6. Geometric parameters (Å, °) for the π···π interactions *.

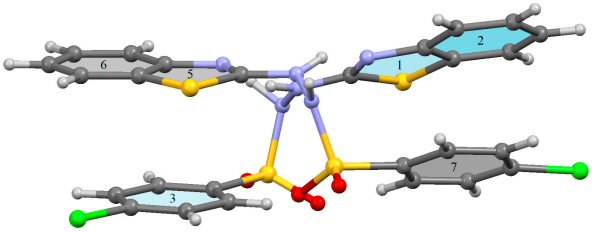

Cpd	Cg(I)···Cg(J)	Cg···Cg	α	CgI_{perp}	CgJ_{perp}	Sym Code	Slippage
1: X = 4-F	Cg2···Cg7	3.9448(15)	9.35(12)	3.4387(10)	3.5588(10)	x, y, z	1.702
	Cg3···Cg5	3.9711(11)	7.95(9)	3.3440(8)	3.5291(8)	x, y, z	1.852
	Cg3···Cg6	4.0113(12)	8.15(10)	3.3376(8)	3.6097(8)	x, y, z	1.749
	Cg6···Cg7	3.9447(15)	9.35(12)	3.3387(10)	3.4387(10)	x, y, z	1.933
	Cg5···Cg7	3.6345(12)	16.76(10)	3.4741(8)	3.5748(9)	$x, y, 1 + z$	0.656
	Cg7···Cg6	3.9187(12)	16.53(11)	3.5720(9)	3.1023(9)	$x, y, -1 + z$	2.394
1: X = 4-Cl	Cg2···Cg7	3.818(2)	3.0(2)	3.4291(16)	3.3890(19)	x, y, z	1.758
	Cg3···Cg5	3.900(2)	0.3(2)	3.4217(17)	3.4267(16)	x, y, z	1.863
	Cg3···Cg6	3.893(3)	1.5(2)	3.4059(17)	3.4530(19)	x, y, z	1.798
	Cg5···Cg7	3.831(8)	29.3(2)	3.4471(16)	3.8135(19)	$x, y, -1 + z$	
1: X = 4-Br	Cg2···Cg7	3.788(3)	2.3(3)	3.410(2)	3.378(2)	x, y, z	1.713
	Cg3···Cg5	3.947(3)	1.9(3)	3.419(2)	3.438(2)	x, y, z	1.938
	Cg3···Cg6	3.909(3)	3.1(3)	3.399(2)	3.498(2)	x, y, z	1.744
	Cg5···Cg7	3.797(3)	28.5(3)	3.385(2)	3.780(2)	$x, y, 1 + z$	
	Cg7···Cg2	3.788(3)	2.3(3)	3.378(2)	3.410(2)	x, y, z	1.649

* See figure in the table for number of the Cg's.

3.3. Hirshfeld Surface Analyses and Fingerprint Plots

Hirshfeld surface analysis has been carried out on compound (**1**: X = F). Figure 3 illustrates views of the surfaces mapped over d_{norm}; the red spots in each of the views correspond to atom···atom close contacts between the reference molecule at x, y, z with its partner molecule in the motif, as defined in the motif list in Table 7 in Section 4.1. The overall FP plots, and the individual atom···atom contacts, which were obtained by partial analysis of the FP plots, are given in Figure 4a,b.

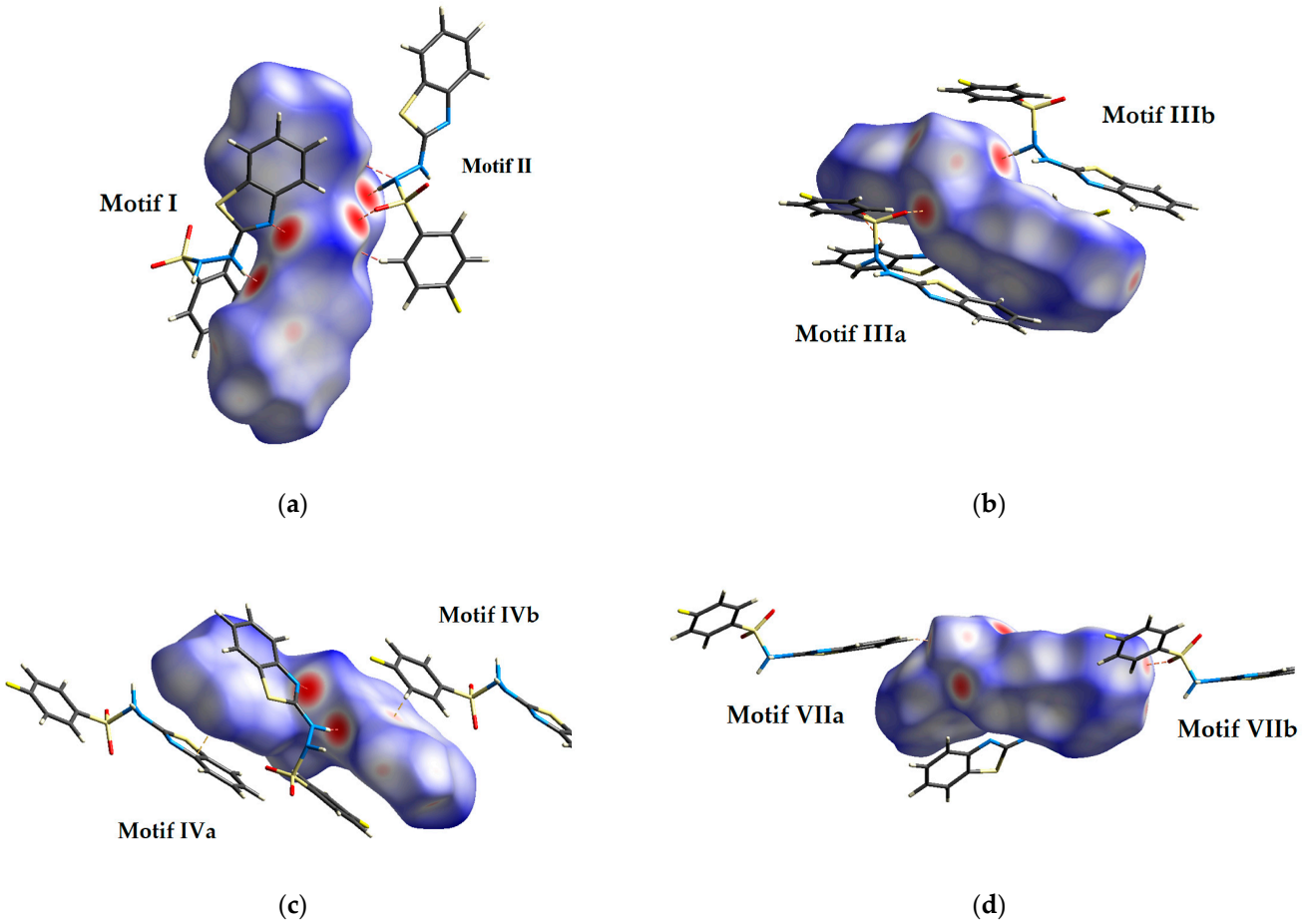

Figure 3. Hirshfeld surface mapped over d_{norm} for (1: X = F) showing red areas that indicate short contacts. (**a**) Motifs **I** and **II**, showing the N221–H221···N13 and the N222–H222···O221 contacts, respectively. (**b**) The chain made by Motifs $\mathbf{III_a/III_b}$, showing the N122–H122···O122 interactions. (**c**) The chain in Motifs $\mathbf{IV_a/IV_b}$ highlighting the π5···π7 interaction and (**d**) Motifs $\mathbf{VII_a/VII_b}$ with the C16–H16···O121 interaction. Refer to Table 4 for geometrical parameters and Table 7 for details of the molecular motifs.

Table 7. List of motifs for compound (**1**: X = F) and their details.

Motif	Symmetry Code	Interactions (Close Contacts)	Distance (Å): Angle (°)	Motif Form	E_{tot}
Motif **I** Mol 1···Mol 2 Asymmetric unit	x, y, z	N121–H121···N23 N221–H221···N13 C124–F124···π6 C224–F124···π2 π2···π7 π3···π5 π3···π6 π5···π3 π6···π3 π6···π7	2.08(3); 165(3) 1.94(3); 165(3) 3.7122(16); 76.07(10) 3.853(2); 71.24(13) 3.9448(15) 3.9711(11) 4.0113(12) 3.9710(11) 4.0112(12) 3.9447(15)	Asymmetric $R^2_2(8)$dimer Figure 6	−120.5
Motif **II** Mol 2···Mol 2	$-x, 1-y, 1-z$	N222–H222···O221 O221···H222–N222	1.88(2); 177(2)	Symmetric dimer: $R^2_2(8)$ Figure 7a	−91.4
Motifs $\mathbf{III_a/III_b}$ Mol 1···Mol 1	$x, 0.5-y, 0.5+z$ $x, 0.5-y, -0.5+z$	N122–H122···O122 C17–H17···π(1)	2.15(3); 168(2) 2.84; 132	C(4) chain Figure 7b	−59.6

Table 7. *Cont.*

Motif	Symmetry Code	Interactions (Close Contacts)	Distance (Å): Angle (°)	Motif Form	E_{tot}
Motifs $\mathbf{IV_a}/\mathbf{IV_b}$ Mol 2···Mol 2	$x, y, 1 + z$ $x, y, -1 + z$	π5···π7 π7···π6	3.6345(12) 3.9187(12)	Chain Figure 7c	−23.9
Motifs $\mathbf{V_a}/\mathbf{V_b}$ Mol 1···Mol 2 Mol 2···Mol 1	$1 - x, 1 - y, 2 - z$	F124···H27	2.68	Pair of acyclic dimers Figure 7d	−21.5
Motif **VI** Mol 2···Mol 2	$1 - x, 1 - y, 2 - z$	C27···H27	2.96	acyclic dimer Figure 7d	−17.1
Motifs $\mathbf{VII_a}/\mathbf{VII_b}$ Mol 1···Mol 1	$1 + x, 0.5 - y, -0.5 + z$ $-1 + x, 0.5 - y, -0.5 + z$	C16–H16···O121 O121···H16–C16	2.44; 162	C(10) chain Figure 7e	−16.2
Motif **VIII** Mol 1···Mol 2	$x, y, -1 + z$ $x, y, 1 + z$	H25···H15	2.20	Pair of H–H contacted dimers Figure 7f	−12.7
Motifs $\mathbf{IX_a}/\mathbf{IX_b}$ Mol 1···Mol 2 Mol 2··· Mol 1	$x, 0.5 - y, 0.5 + z$ $x, -y, -0.5 + z$	C24–H24···O121	2.55; 138	Two pairs of acyclic dimers Figure 7b	−11.9

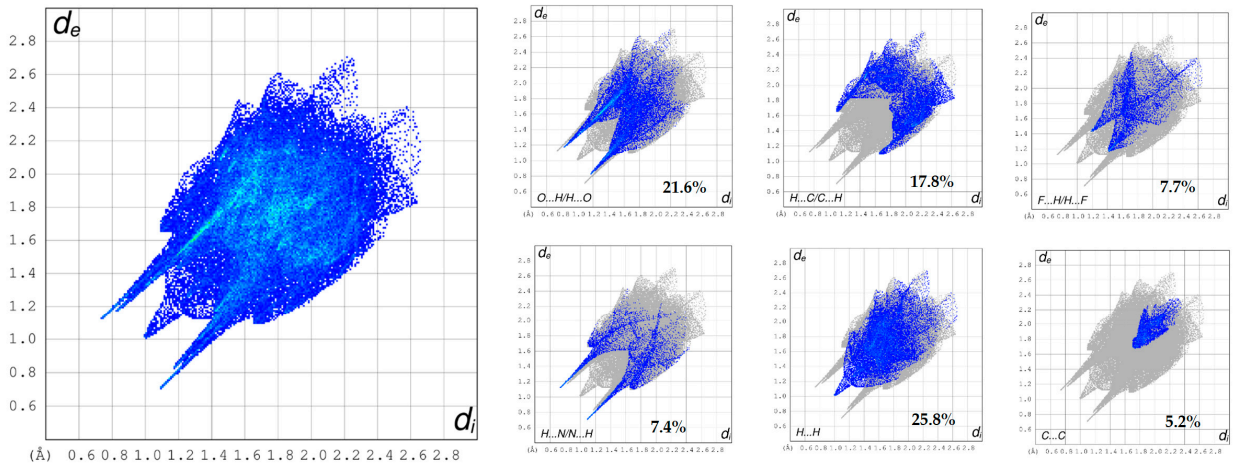

(**a**)

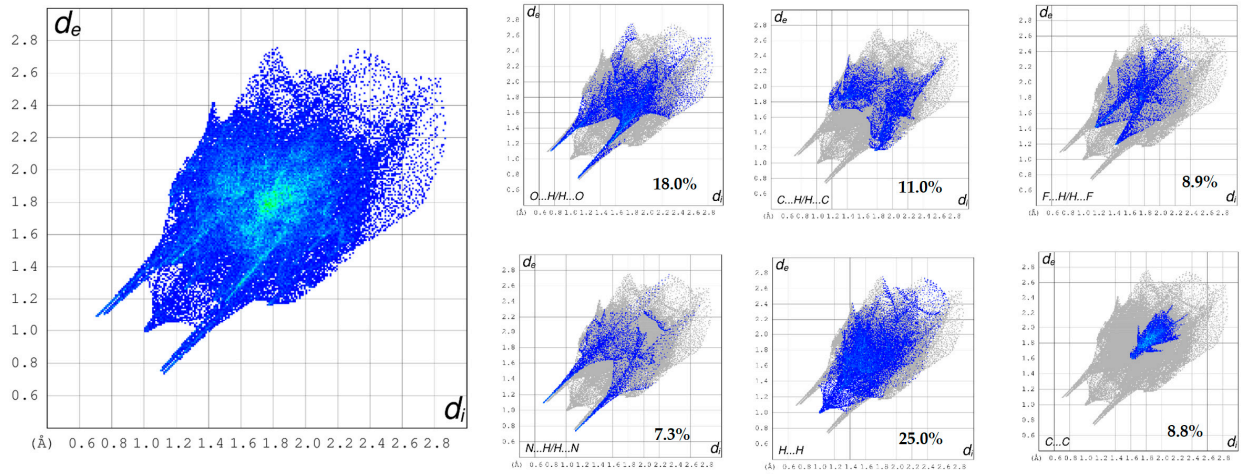

(**b**)

Figure 4. (**a**).Finger print plots for **1:** X = 4-F, Mol 1. (**b**) Finger print plots for **1**: X = 4-F, Mol 2.

*3.4. Calculated Energies for (**1**: X = 4-F)*

The mean total energy for the lattice, E_{tot}, per molecule obtained using PIXEL [42,43], was −189.3 kJ.mol^{-1} distributed as follows: −140.5,−69.8,−184.9, and 205.9 kJ.mol^{-1} for E_c, E_{pol}, E_{disp}, and E_{rep}, respectively. The calculations allowed the identification of the nine molecular pairs (motifs **I** to **IX**) (see Table 7) that were considered the most significant, i.e., those with $-E_{tot}$ values greater than 10 kJ.mol^{-1}. The graphic representation of Figure 5 shows how the total energies for each motif are distributed.

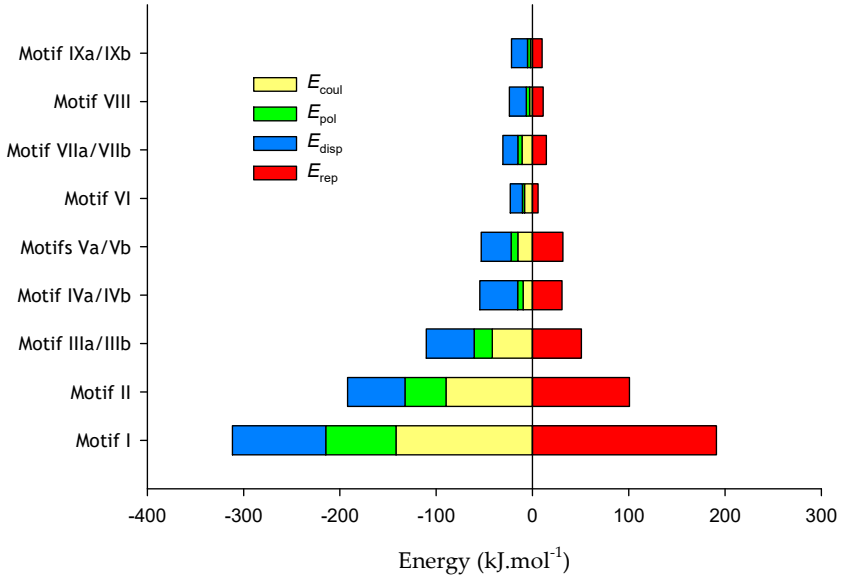

Figure 5. E_{coul}, E_{pol}, E_{disp} and E_{rep}, for the lattice motifs I–IX found in **1**: X = 4-F.

Other details provided in Table 7 include the symmetry operations, intermolecular interactions, geometric parameters, and forms of the motif, i.e., chain or dimer (acyclic or cyclic). Individual motifs involve two molecules; thus, the energy per mol is a half of the motif's energy. Furthermore, in a chain of motifs, the reference molecule at x, y, z is common to two motifs, motif ZA and motif ZB, each of equal energy. The listing of motifs for each compound in Table 7 is given in decreasing order of $-E_{tot}$ values. The motifs can be viewed in Figures 6 and 7a–f.

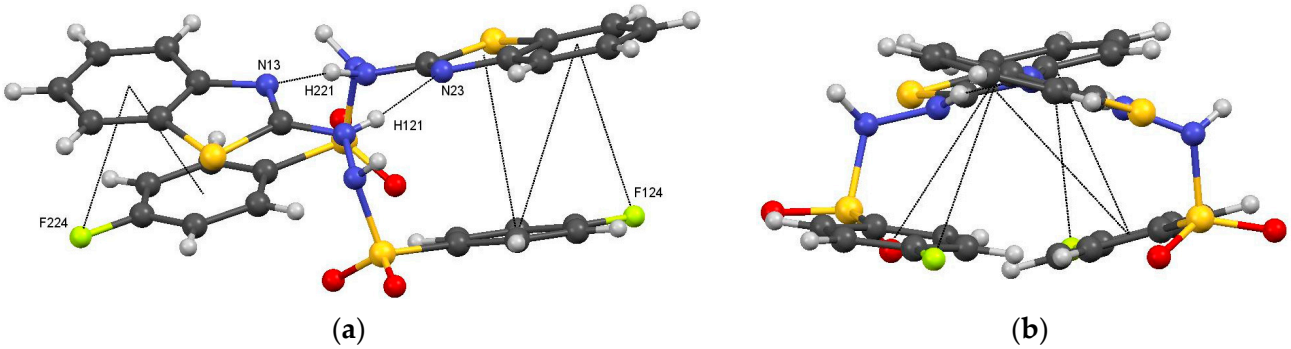

Figure 6. Compound (**1**: X = F): Motif **I**. Two representations of motif **I**, (**a**) a dimer formed from Mol 1 and Mol 2 in the asymmetric unit, (**b**) one formed by N121–H121···N23 and N221–H221···N13 hydrogen bonds and C124–F124···π6 and C224–F124···π2 interactions, and one with a series of face-to-face, offset π···π interactions [for ring numbers, see Tables 5–7].

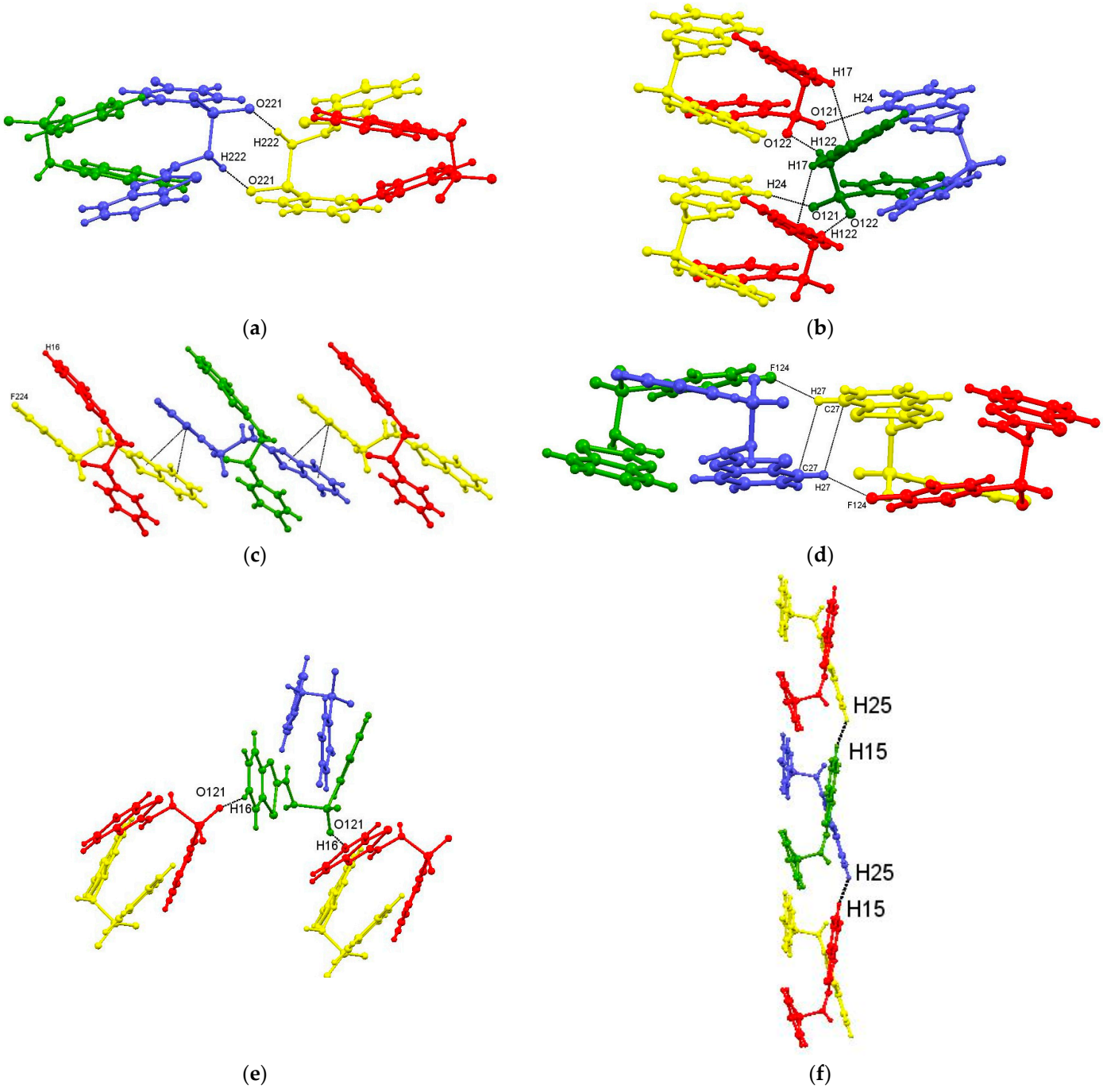

Figure 7. (**a**) Motif **II** (colours: blue & yellow; (**b**) Motifs $\mathbf{III_a}$ & $\mathbf{III_b}$ (chain: red, green, & red); motifs $\mathbf{IX_a}$ & $\mathbf{IX_b}$ (red & blue and yellow & green); (**c**) Motifs $\mathbf{IV_a}$ & $\mathbf{IV_b}$ (chain: colours yellow, blue, & yellow); Motifs $\mathbf{VII_a}$ & $\mathbf{VII_b}$ (colours red, green, & red); motifs **I**: (colours: green and blue at *x*, *y*, *z* and red & yellow). (**d**) Motifs $\mathbf{V_a}$ & $\mathbf{V_b}$ (colour: green & yellow, and red & blue)and motif **VI** (yellow & blue); (**e**) Motifs $\mathbf{VII_a}$ & $\mathbf{VII_b}$ (colours red, green, & red); (**f**) Motifs $\mathbf{VIII_a}$ & $\mathbf{VIII_b}$ (green & yellow and red & blue). Motifs **I** (green & blue, at *x*, *y*, *z* and red & yellow).

4. Discussion

4.1. Molecular Structures

All the hydrazide molecules are in the amino tautomer form, with Cx2-Nx2 bonds distances ranging from 1.343(3) to 1.364(6); see Table 4), suggesting a delocalization of the electronic cloud within the C-NH-NH-S-linker. Similar results are apparent from other already published structures with the same linker [48–50].

Some molecules exhibit intramolecular C–H···O hydrogen bonds, which are drawn as dashed lines in Figure 2. In those H bonds, the oxygen atom of the sulphonyl acts as an acceptor for the H atom of the Ph ring, forming a S5 ring (see Table 5 for geometric parameters). Views looking down the best planes through both the benzothiazol and phenyl groups show in all cases a conformation between "U"- and "J"-shaped structures (see Figure 2). The interplanar angles between the benzothiazol and phenyl groups are close to 30° for all molecules except Mol 2 of compound (**1**: X = F), which contains a considerably smaller angle of 16.6°.

This and other parameters, which are listed in Table 6, illustrate the small differences between the two independent molecules for each compound, as well as differences amongthe three compounds, with the exception of Mol 2 of (**1**: X = F). Differences in the conformations of the molecules in (**1**: X = F, Cl and Br) can be assessed by torsion angles: thereare 10° differences in the torsional C22-N221-N222-S22 angles in Mol 2 of (**1**: X = F) compared with those in Mol2 of (**1**: X = Cl and Br), and there are also differencesin the interplanar angle between the Ph and Bt rings: 17° for Mol 2 of (1: X = F) compared to ca 30° for (**1**: X = Cl and Br). This difference could be attributed to the different sizes of the halogen units.

4.2. Crystal Structures

Among the intermolecular interactions found by PLATON [40] for the three compounds are N–H···N, N–H···O, C–H···O, C–H···F, C–H···Cl, and C–H···Br hydrogen bonds, as well as face-to-face, offset π···π, C–H···π, and C–X···π (X = F, Cl and Br) interactions. In contrast to (1: X = O_2N) compounds [32], SO2···π interactions are not present, although N–H···O (sulfone) and C–H···O (sulfone) hydrogen bonds are present.

4.2.1. Supramolecular Motifs and Lattice Energies for **1**: X = 4-F

The combination of the analysis of the HS (plotted by d_{norm}) with the information given by PLATON concerning the geometry of classic hydrogen bonds, the Y–X···π interactions, and the π···π interactions allows the identification of the relevant intermolecular interactions that form the crystal structure. The normalized contact distance, d_{norm}, a symmetric function of distances to the surface from nuclei inside, d_i, and outside, d_e, relative to the appropriate *van der Waals* radius, when plotted on the Hirshfeld surface, allows important regions for close contacts to be identified: d_{norm} is shown in red in regions where the contacts are closer than the sum of *van der Waals* radius, thus corroborating the results obtained for the interactions in PLATON and helping in the identification of lattice motifs. Derived from the Hirshfeld surface, the 2D-fingerprint plots give a visual summary of the frequency of each combination of d_e and d_i across the surface of a molecule. In the partial fingerprint plots are the identification and quantification of specific intermolecular interactions. The PIXEL calculations allow the selection of those motifs that contribute the most, in terms of energy, to the stabilization of the lattice. All of this combined information is given in Table 7 and will be used in the discussion.

Intermolecular Contacts in **1**: X = F

All N and O atoms of Mol1 and Mol2 are involved in H bonds, with the exception of O222 of Mol2. As expected, the slight differences in the conformations of the two

independent molecules, Mol 1 and Mol 2, result in differences in the specific percentage of atom···atom contacts. The FP analysis reveals that there are some differences in the frequency of close contacts between the two molecules: the C···H and O···H contacts are more common in Mol1, while Mol2 has a higher percentage of C···H and C···C contacts (see Figure 4a,b). The percentage of H···H contacts isca.25%, a value lower than that expected for organic molecules.

The PIXEL calculations provided a more extensive structural study and showed that there are several molecule pairs/motifs with $-E_{tot}$ less than 10.0 kJ.mol^{-1}. The interactions on which the structural motifs are based were confirmed on the HS; Figure 3a–d shows that the HS allowed the identification of motifs **I**, **II**, and **IV** and the pairs associated with motifs **III** and **VII**, where the strong N···H and O···H H bonds can be identified by the intense red spots.

1: X = F Motifs

Motif **I** is composed of the two molecules in the asymmetric unit and is by far the most significant motif (Figure 6). The contacts between Mol 1 and Mol 2 involve N–H(hydrazinyl)···N(thiazolyl) hydrogen bonds, C–H(phenyl)···π(phenyl) interactions, and face-to-face, off-set π···π interactions (see Tables 4–7). Motif **I** is in the form of an dimer containing a R22(8) ring formed from N121–H121···N23 and N221–H221···N13 classical hydrogen bonds. The combination of the different intermolecular contacts produces a strong motif with a total energy of −120.5 kJ.mol^{-1}. That energy is made up of the component terms E_{Coul}, E_{pol}, and E_{disp}, which have values of −141.8, −72.9, and −96.7 kJ, respectively (see Figure 5),and those negative values are offset by the E_{rep} value of 190.9 kJ mol^{-1}. The strong classical N–H···N hydrogen bonds contribute greatly to the high values of the E_{Coul} and E_{pol} components, and the π interactions contribute greatly to the E_{disp} value. Thus, in spite of the presence of several π···π interactions, the H···NH bonds account for most of the total stabilization energy of the lattice. As indicated in a recent report on the isomeric derivatives Bt-NHNHSO$_2$C$_6$H$_4$NO$_2$ -o,-m and -p [32], the most important motifs in each compound have R22(8) dimeric arrangements similar to that now reported here. For the motifs **I** of the nitro derivatives, classical N–H(hydrazinyl)···N(thiazolyl) hydrogen bonds, and face-to-face, off set π···π interactions were also generally present. Compared to (1:X = F), the motifs **I** of the nitro derivatives had higher $-E_{tot}$ values (142–164 kJ mol^{-1}).

Motifs **II**–**IX** have much lower energies than motif **I**, for example the range of $-E_{tot}$ values for motifs **II**–**IX**, are 11.9 to 91.4 kJ.mol^{-1}, while the ranges of the component energies, $-E_{Coul}$, $-E_{pol}$ and $-E_{disp}$ are 2.1–89.8, 2.2–42.6 and 12.5–59.6 kJ.mol^{-1}, respectively (see Figure 3) Of interest, each of the motifs **II** to **IX** bridge motif **I** via contacts with either or both the molecules in motif **I**, and, as such, they extend the aggregation of motif **I** from a dimer to layers and infinite columns.

The component values of the energies in motifs **II** and **III,** while not as large as those in motif **I**, are still significant (see Figure 5).These significant component values arise despite differences in the types of contacts linking the motifs: motif **II**, a symmetrical dimer with a R22(8) ring, is formed from a pair of N222–H222(hydrazinyl)···O221(sulfone) classical hydrogen bonds (see Figure 7a), is composed of two Mol 2 units, while in motifs **III$_a$** and **III$_b$** (Figure 7b), the Mol 1 chain is linked by a combination of a classical N122–H122···O122(sulfone) hydrogen bond and a C17–H17···π(thienyl) interaction. The $-E_{Coul}$ and $-E_{pol}$ values for motif **II** are large, at 89.8 and 42.6 kJ.mol^{-1}, respectively, and those for motif **III** are approximately half these values, at −41.6 and 18.9 kJ.mol^{-1} (see Figure 5).These values are as expected for motifs with the classical hydrogen-bonded contacts they possess. However, the $-E_{disp}$ value for motif **II** is rather large, at 59.6 kJ.mol^{-1}, considering there are no π-type interactions linking the molecules in the motif. As mentioned above, and as shown in Figure 7, motifs **II** to **IX** are all linked, albeit in different

ways, to motif **I** molecules, and so electron delocalisation could arise between motif **I** and motif **II.** This delocalisation could account for the E_{disp} in the molecular pair. In a similar way, motifs **III$_a$/III$_b$** also present a relatively high value for $-E_{disp}$ (49.8 kJ.mol^{-1}), which appears high for C17–H17···π(thienyl) interactions, leading to the possibility that, beyond this π interaction, significant delocalisation involving connections to motif **I** contribute to the E_{disp}.

The remaining motifs, **IV** to **IX**, have $-E_{tot}$ values less than 25 kJ.mol^{-1}, and all have -E_{disp} components as the largest contributor to $-E_{tot}$: this pattern holds regardless of whether or not there are face-to face, offset π···π interactions, as in motifs **IV$_a$** and **IV$_b$** (and thus as anticipated) or just C–H···O hydrogen bonds (as in motifs **VII$_a$**/**VII$_b$** and **IX$_a$**/**IX$_b$**, and thus not as expected), or indeed whether the closest contacts between the molecule pairs in the motif simply involve atoms at the limit of, or indeed outside, the contact radii sum (as in motifs **V$_a$**/**V$_b$**, **VI** and **VIII**). Again, electronic delocalisation is here considered to occur to some extent between these motifs and motif **I**.

4.2.2. Intermolecular Interactions in (**1**: X = Cl) and (**1**: X = Br)

Those compounds form an isostructural pair. As said before, the X-ray data collected for (**1**: X = Cl) and (**1**: X = Br) made the structural determination of the molecules possible, but the presence of disordered solvent (water) molecules that could not be positioned accurately (but that certainly do interact with the main molecules) make both HS analysis and PIXEL analysis impossible. Thus, only PLATON analysis was conducted, and the information thus obtained on the intermolecular interactions in the (**1**: X = Cl) and (**1**: X = Br) is given in Tables 4–6. Comparison of the intermolecular interactions found in (**1**: X = F) with those identified in (**1**: X = Cl) and (**1**: X = Br) allowed identification of related molecule pairs in the three compounds. However, without knowledge of the energies of these molecule pairs in (**1**:X = Cl) and (**1**: X = Br), their importance and ranking in terms of energy values cannot be obtained. Comparisons of the intermolecular interactions in (**1**: X = F), with those identified in (**1**: X = Cl) and (**1**: X = Br) indicate the following(see Table S4 for details):

- the motifs of type **I** in (**1**: X = F), with N121–H121···N23 and N221–H221···N13 hydrogen bonds, C124–X···π6 interactions, and face-to-face offset π···π interactions, have equivalents in (**1**: X = Cl and Br),
- the motifs of type **III** in (**1**: X = F), with N122–H122···O122 hydrogen bonds and C17–H17···π(1), have equivalents in (**1**: X = Cl and Br),
- the motifs of type **IV** in (**1**: X = F), with face-to-face, offset π···π interactions have equivalents in (**1**: X = Cl and Br),
- the interactions present in the weaker, lower-energy motifs, **IV** to **IX**, in (**1**: X = F), were not identified by PLATON in (**1**: X = Cl and Br),
- the equivalent of motif **II** in (**1**: X = F) is not present in (**1**: X = Cl and Br). The links between the molecules in motif **II** in (**1**: X = F) are a pair of N222–H222···O221 hydrogen bonds, while in (**1**: X = Cl and Br), the N222–H222 atoms, while not confirmed, are apparently hydrogen bonded to disordered water molecules residing in voids in the crystal structure.

However, there is one type of π-interaction specific to the (**1**: X = Cl and Br) pair: this interaction involves C26–H26···X1 hydrogen bonds that link molecules into acyclic dimers: Figure 8 shows several of these links, along with their contacts with motif **I**. We do not think that these C26–H26···X1 hydrogen bonds will provide the substantial energy needed to overcome the loss arising from the absence of any N222–H222 interaction in (**1**: X = Cl or Br). The packing diagrams for (**1**: X = Cl), in Figure 9a,b are similar to that obtained for (**1**: X = Br).

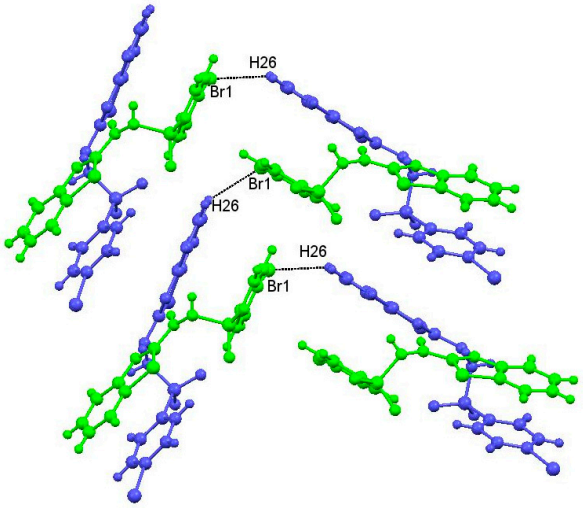

Figure 8. The C25–H26···Br1 interactions in (**1**: X = Br). A similar interaction is present in (**1**: X = Cl).

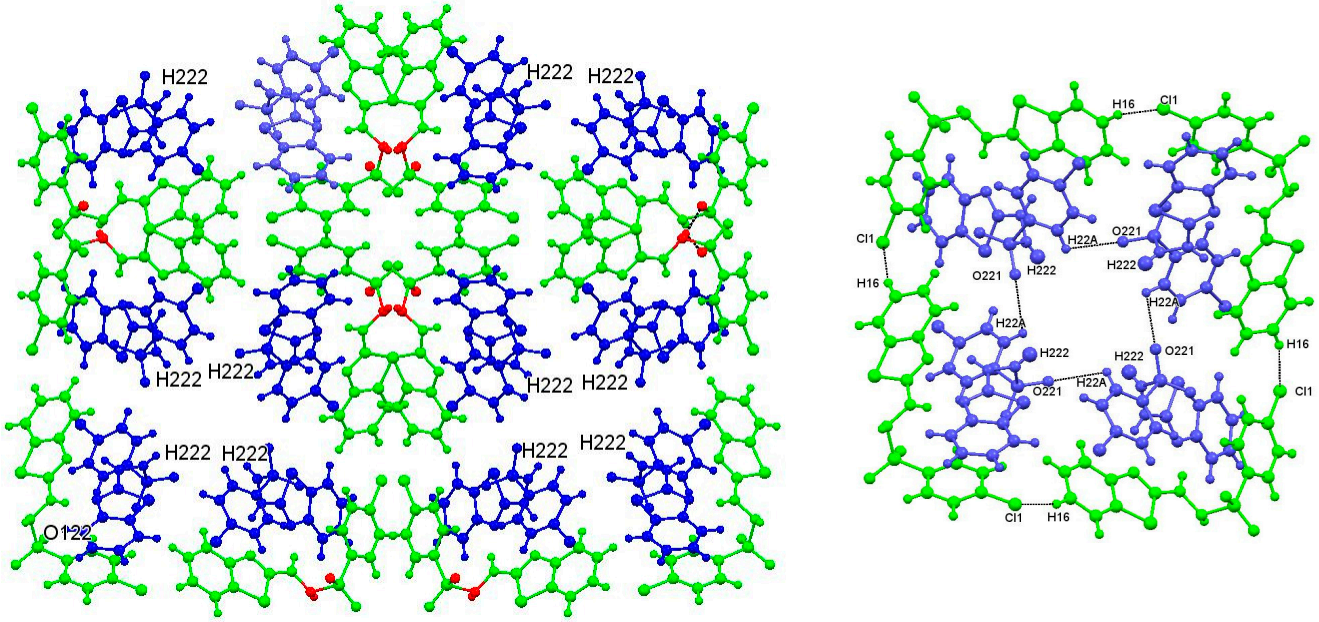

(**a**) (**b**)

Figure 9. Packing of molecules of compound (**1**: X = Cl); (**a**) a view of the packing looking down the *c* axis; atoms in Mol 1 and Mol 2 are drawn in green and blue, respectively; atoms drawn in red are involved in the N122–H122···O122 hydrogen bonds; (**b**) a more detailed view of the 4-fold symmetric arrangement, encompassing four H222 sites, again looking down the *c* axis. Four H222 hydrogens are oriented into the void, which forms on the removal of disordered solvent (water) molecules.

4.3. Related Compounds

The substituted N-(1,3-benzothiazol-2-yl)-benzenesulfonylhydrazides(**1**) both those studied here, (**1**: X = F, Cl and Br) and those previously reported (**1**: X = H) [31] and (**1**: X = O_2N) [32], have E_{disp}, E_{Coul} and E_{pol} values that make strong contributions to the overall stability of the compounds. These values arise from each compound's sets of face-to-face, offset π···π interactions involving the Bt and phenyl aromatic groups and strong classical hydrogen bonds. In the discussion that follows, in Mol 1 and Mol 2, the hydrazinylnitrogens bonded to the benzothiazolyl groups are numbered N121 and N221, those bonded to the sulfone sulphur atoms are N122 and N222, and the thienyl nitrogens in the benzothiazolyl ring are N13 and N23.

The hydrazinyl NH units, N121–H121 and N221–H221, invariably form hydrogen bonds with the thienyl nitrogens, N13 and N23, in all the compounds of type**1** studied so far. The thienyl nitrogens, N122 and N222, are more flexible in making connections to any potential acceptor, such as nitro and sulfonyl oxygens. Thus, in (**1**: X = H), which contains a substituent, H, possessing no acceptor properties, N122–H122(hydrazinyl)···O(sulfonyl) and N222–H222(hydrazinyl)···O(sulfonyl) hydrogen bonds are formed, as the sulfonyl oxygens are the only available strong acceptors; weaker C–H···O(sulfonyl) hydrogen bonds are also present.

For compounds (**1**: X = 2-O_2N, 3-O_2N, and 4-O_2N), different situations pertain due to the nitro-group oxygens being strong competitors with the sulfonyl oxygens as acceptors. Furthermore, the positions of the nitro groups in the phenyl ring are important. The location of the nitro group in (**1**: X = 2-O_2N) allows the formation of intramolecular N122–H122(hydrazinyl)···O(nitro) and N222–H222(hydrazinyl)···O(nitro) hydrogen bonds, rather than intermolecular ones; the sulfonyl oxygens are involved only in weaker C–H···O bonds. In compounds (**1**: X = 3-O_2N) and (1: X = 4-O_2N), in whichthe nitro groups are more remote from the hydrazinyl NH units, the N122–H122(hydrazinyl) and N222–H222(hydrazinyl) now form intermolecular hydrogen bonds with the nitro oxygen atoms, O13 and O23, respectively. Again, the sulfonyl oxygens are here relegated to forming weaker C–H···O hydrogen bonds. For the well-ordered compound (**1**: X = F), formations of both N122–H122(hydrazinyl)···O122(sulfonyl), and N222–H222(hydrazinyl)···O221(sulfonyl) are clearly confirmed. These interactions involve two Mol 1 and two Mol 2 molecules, respectively. The disorder in (**1**: X = Cl and Br) prevented the performance of studies to confirm the identity of connections to the N222–H222(hydrazinyl) unit. However, the formations of the N122–H122(hydrazinyl)···O122(sulfonyl) hydrogen bonds in (**1**: X = Cl and Br were securely established and again were shown to involve two Mol 1 molecules.

As shown by PIXEL calculations for compound (**1**: X = F),the energy contributions gained from the N221-H221(hydrazinyl) and N222-H222(hydrazinyl) contacts are considerable, and the loss of one such interaction would have serious energy consequences if it were not fully compensated. The C26–H26···X1 (X = Cl and Br) hydrogen bonds found in (**1**: X = Cl and Br) but absent from (**1**: X = F) are not expected to make sufficiently strong contributions. On looking at the packing diagram for (**1**: X = Cl) (see Figure 9), there are no alternative acceptors, including nearby aromatic groups, to form contacts. NB: as(**1**: X = Cl) and (1: X = Br) are isostructural, a similar situation pertains for the bromo analogue, which is not thus shown. Thus, we surmise that in Mol 2 in both (**1**: X = Cl) and (**1**: X = Br), the N222-H222 (hydrazinyl) units is likely to make contacts with the disordered water molecules within the void and thereby result in the formation of potential N222-H222(hydrazinyl)···O(aqua) hydrogen bonds.

5. Conclusions

The dominance of the dimers formed from the two independent molecules in all three compounds is an important finding. While disorder prevented Hirshfeld and PIXEL analyses of the chloro and bromo structures and consequently prevented the collection of information on the molecular pairs, the PLATON analyses strongly indicate that there are generally similar intermolecular interactions within the dimers of all three compounds, with very strong and common intra-motif N–H(hydrazinyl)···N(thiazolyl) hydrogen bonds and sets of face-to-face $\pi\cdots\pi$ interactions. Such findings have been found for three isomer nitro derivatives and the parent compound, BtNHNHSO_2Ph. For all these compounds, the importance of these dimeric sub-structures is further emphasized bytheir linkage in other interactions to form higher aggregates.

Two inconsistent findings have been found in these structural studies of the BtNHNHHHSO_2Ar compound family: (i) the reaction between BtNHNH_2 and X$C_6H_4SO_2$Cl, for X = 4-I produces the isomeric product, BtNHN(S$O_2C_6H_4$I)NH_2, in contrast to all other reactions, which lead to products BtNHNHS$O_2C_6H_4$X, and (ii) the lack of a ordered acceptor for the N222-H222(hydrazonyl) fragment in the isostructural chloro and bromo structures

(e.g., sulfonate oxygen), as was found in the fluoro case. For (i), a pre-reaction iodo/phenyl interaction was initially indicated, but the possibility of a steric effect from the iodo group remains, and for (ii), the sizes of the chloro and bromo groups are considered possible factors. While allowing the more stabilizing combination of -H(hydrazinyl) ···N(thiazolyl) hydrogen bonds and face-to-face π···π interactions to occur, steric effects prevent the less significant single N222-H222(hydrazonyl) ···O(sulfonate) hydrogen bonds from forming. Further studies are planned to investigate steric effects and pre-reaction interactions of other substituent groups.

Supplementary Materials: The following supporting information can be downloaded at: https://www.mdpi.com/article/10.3390/cryst14040330/s1, Table S1: Crystal data for compounds; Table S2: Selected Torsion angles (°). Table S3: Geometric parameters (Å, °) for the π···π interactions. Table S4: Assumed molecular pairs formed from intermolecular interactions in compounds (**1**: X = Cl and Br) on comparisons with confirmed interactions in (**1**: X = F).

Author Contributions: Conceptualization, J.L.W. and L.R.G.; methodology, J.L.W. and A.C.P.; software, J.N.L. and L.R.G.; validation, J.N.L., L.R.G. and J.L.W.; investigation, J.L.W., L.R.G. and A.C.P.; resources, J.L.W.; writing—original draft preparation, J.L.W.; writing—review and editing, L.R.G. and J.N.L.; supervision, J.L.W. All authors have read and agreed to the published version of the manuscript.

Funding: This research received no external funding.

Data Availability Statement: Full structural data can be find in https://www.ccdc.cam.ac.uk/structures/; CCDC numbers 2124146; 2193760; 2123875.

Acknowledgments: The authors thank the staff at the National Crystallographic Service, University of Southampton, for the data collection, help and advice.

Conflicts of Interest: The authors declare no conflicts of interest.

References

1. Heijstek, A. *Benzothiazole: Preparation, Structure and Uses*, 1st ed.; Nova Science Publishers Inc.: New York, NY, USA, 2020.
2. Elamin, M.B.; Elaziz, A.A.E.S.A.; Abdallah, E.M. Benzothiazole moieties and their derivatives as antimicrobial and antiviral agents: A mini-review. *Int. J. Res. Pharm. Sci.* **2020**, *11*, 3309–3315. [CrossRef]
3. Pathak, N.; Rathi, E.; Kumar, N.; Kini, S.G.; Rao, C.M. A Review on Anticancer Potentials of Benzothiazole Derivatives. *Mini Rev. Med. Chem.* **2020**, *20*, 12–23. [CrossRef] [PubMed]
4. Asif, M.; Imran, M. A Mini-Review on Pharmacological Importance of Benzothiazole Scaffold. *Mini Rev. Org. Chem.* **2021**, *9*, 1086–1097. [CrossRef]
5. Abrol, S.; Bodla, R.B.; Goswami, C. A comprehensive review on benzothiazole derivatives for their biological activities. *Int. J. Pharm. Sci. Res.* **2019**, *10*, 3196–3209.
6. Keri, R.S.; Patil, M.R.; Patil, S.A.; Budagumpi, S.A. Comprehensive Review in Current Developments of Benzothiazole-Based Molecules in Medicinal Chemistry. *Eur. J. Med. Chem.* **2014**, *89*, 207–251. [CrossRef] [PubMed]
7. Law, C.S.W.; Yeong, K.Y. Current trends of benzothiazoles in drug discovery: A patent review (2015–2020). *Exp. Opin. Ther. Pat.* **2022**, *32*, 299–315. [CrossRef] [PubMed]
8. Gjorgjieva, M.; Kikelj, T.D.; Masic, L.P. Benzothiazole-based Compounds in Antibacterial Drug Discovery. *Curr. Med. Chem.* **2018**, *25*, 5218–5236. [CrossRef]
9. Maliyappa, M.R.; Keshavayya, J.; Mallikarjuna, N.M.; Pushpavathi, I. Novel substituted aniline based heterocyclic dispersed azo dyes coupling with 5-methyl-2-(6-methyl-1, 3-benzothiazol-2-yl)-2, 4-dihydro-3H-pyrazol-3-one: Synthesis, structural, computational and biological studies. *J. Mol. Struct.* **2020**, *1205*, 127576. [CrossRef]
10. Thekkeppat, N.P.; Lakshmipathi, M.; Jalilov, A.S.; Das, P.; Malik, A.; Peedikakkal, P.; Ghosh, S. Combining Optical Properties with Flexibility in Halogen-Substituted Benzothiazole. *Cryst. Growth Des.* **2020**, *20*, 3937–3943. [CrossRef]
11. Nootem, J.; Daengnern, R.; Sattayanon, C.; Wattanathana, W.; Wannapaiboon, S.; Rashatasakhon, P.; Chansaenpak, K. The synergy of CHEF and ICT toward fluorescence 'turn-on' probes based on push-pull benzothiazoles for selective detection of Cu^{2+} in acetonitrile/water mixture. *J. Photo. Chem. Photobiol. A Chem.* **2021**, *415*, 113318. [CrossRef]
12. Foo, K.-L.; Ha, S.-T.; Yeap, G.-Y. Synthesis and phase transition behavior of calamitic liquid crystals containing heterocyclic core and lateral ethoxy substituent. *Phase Trans.* **2002**, *95*, 178–192. [CrossRef]
13. Lioa, C.; Kim, U.J.; Kannan, K. A Review of Environmental Occurrence, Fate, Exposure, and Toxicity of Benzothiazoles. *Environ. Sci. Technol.* **2018**, *52*, 5007–5026. [CrossRef] [PubMed]

14. Le Bozec, L.; Moody, C.J. Naturally Occurring Nitrogen–Sulfur Compounds. The Benzothiazole Alkaloids. *Aust. J. Chem.* **2009**, *62*, 639–647. [CrossRef]
15. Khalil, M.I.; Khalal, Q.Z. Synthesis and characterization of new compounds derived from 2-hydrazinobenzothiazole and evaluated their antibacterial activity. *J. Phys. Conf. Ser.* **2021**, *1853*, 012007. [CrossRef]
16. Badr, M.Z.A.; Mahmoud, A.M.; Mahgoub, S.A.; Hozien, Z.A. Condensation and Cyclization Reactions of 2-Hydrazinobenzimidazole, -benzoxazole, and -benzothiazole. *Bull. Chem. Soc. Jpn.* **1988**, *61*, 1339–1344. [CrossRef]
17. Elsayed, S.A.; Saad, E.A.; Mostafa, S.I. Development of New Potential Anticancer Metal Complexes Derived from 2-Hydrazinobenzothiazole. *Mini Rev. Med. Chem.* **2019**, *19*, 913–922. [CrossRef] [PubMed]
18. Gomes, L.R.; Low, J.N.; Pinheiro, A.C.; de Souza, M.V.N.; Wardell, J.L. Crystal structure, Hirshfeld surface analysis and PIXEL calculations of the three isomeric (E)-2-((pyridinylmethylidene)hydrazinyl)benzo[d]thiazoles: Occurrence of stacking interactions. Journal of Molecular Structure. *J. Mol. Struct.* **2021**, *1230*, 129907. [CrossRef]
19. Nogueira, A.; Vasconcelos, T.R.A.; Wardell, J.L.; Wardell, S.M.S.V. Crystal structures of hydrazones, 2-(1,3-benzothiazolyl)-NH—N=CH—Ar, prepared from arenealdehydes and 2-hydrazinyl-1,3-benzothiazole. *Z. Für Krist.* **2011**, *226*, 846–860. [CrossRef]
20. Lindgren, E.B.; Yoneda, J.D.; Leal, K.Z.; Nogueira, A.F.; Vasconcelos, T.R.A.; Wardell, J.L.; Wardell, S.M.S.V. Structures of hydrazones, (E)-2-(1,3-benzothiazolyl)-NHNCHAr, [Ar=4-(pyridin-2-yl)phenyl, pyrrol-2-yl, thien-2-yl and furan-2-yl]: Difference in conformations and intermolecular hydrogen bonding. *J. Mol. Struct.* **2013**, *1036*, 19–27. [CrossRef]
21. Hünig, S.; Kaupp, G. Azofarbstoffedurchoxydativekupplung—XXVIII: Kinetik der kupplungheterocyclischer carbonyl- und sulonylazo-quartärsalzemitphenolenzudiazamerocyaninen. *Tetrahedron* **1967**, *23*, 1411–1439. [CrossRef]
22. Hünig, S.; Kießlich, G.; Oette, K.-H.; Quast, H. AzofarbstoffedurchoxydativeKupplung, XXIX. Derivate der 3-Methyl-1.2-benzisothiazolon-(2)-, 1.3-Benzdithiolon-(2)- und 1.2-Benzdithiolon-(3)-hydrazone. *Justus Liebigs Ann. Chem.* **1972**, *754*, 46–55. [CrossRef]
23. Agfa-Gevaert-AG. Sulphonylamidrazone Prepn–Single Stage Process Using Oxidation Agents. DE2105063 A1, 24 August 1972.
24. HENKEL ag & Co. KGAA. Sulfonylhydrazines, Metal Complexes Thereof, and Solutions Containing such Compounds for Use in Extraction of Metal Values. USA 4252959, 13 October 1981.
25. Institut khimiko-fotograficheskoj promyshlennosti. Method of Preparing Heterocyclic Sulfonyl- or Acylhydrazones1. SU702016A1, 5 December 1979.
26. EISAI Co., Ltd. A1 Aryl and Heteroaryl Compounds Useful as Fibroblast Growth Factor Antagonists. WO2000/30632, 2 June 2000.
27. Norman, D.D.; Ibezim, A.; Scott, W.E.; White, S.; Parrill, A.L.; Baker, D.L. Autotaxin inhibition: Development and application of computational tools to identify site-selective lead compounds. *Bioorg. Med Chem.* **2013**, *21*, 5548–5560. [CrossRef] [PubMed]
28. Li, X.; Shan, J.; Chang, W.; Kim, I.; Bao, J.; Lee, H.J.; Zhang, X.; Samuel, V.T.; Shulman, G.I.; Liu, D.; et al. Chemical and genetic evidence for the involvement of Wnt antagonist Dickkopf2 in regulation of glucose metabolism. *Proc. Natl. Acad. Sci. USA* **2012**, *109*, 11402–11407. [CrossRef] [PubMed]
29. Noha, S.M.; Jazzer, B.; Kuehni, S.; Rollinger, J.M.; Stuppner, H.; Schaible, A.M.; Wetz, O.; Wolber, G.; Stupper, D. Pharmacophore-based discovery of a novel cytosolic phospholipase A2α inhibitor. *Bioorg. Med. Chem. Lett.* **2012**, *22*, 1202–1207. [CrossRef] [PubMed]
30. Peretyazhko, M.Z.; Pel'kis, P.S. Unsymmetrically substituted benzothiazolyl-hydrazines. *Chem. Heterocycl. Compd.* **1971**, *7*, 713–714. [CrossRef]
31. Baddeley, T.C.; de Souza, M.V.N.; Wardell, J.L.; Jotani, M.M.; Tiekink, E.R.T. N′-(1,3-Benzo thia zol-2-yl) benzene sulfono hydrazide: Crystal structure, Hirshfeld surface analysis and computational chemistry. *Acta Crystallogr. Sect. E Crystallogr. Commun.* **2019**, *E75*, 523–526.
32. Gomes, L.R.; Low, J.N.; Pinheiro, A.C.; Wardell, J.L. Crystal packing of structurally similar and strong dimeric subunits of isomeric N/-(1,3-benzothiazol-2-yl)nitrobenzenesulfonylhydrazides, influenced by the position of the nitro group. *J. Mol. Struct.* **2024**, *1298*, 136957. [CrossRef]
33. Gomes, L.R.; Fruchtl, H.; Low, J.N.; van Mourik, T.; Pinheiro, A.C.; de Souza, M.V.N.; Wardell, J.L. Crystal structure of N-(1,3-benzothiazol-2-yl)-4-iodobenzene-1-sulfonohydrazide: The unexpected importance of l N-H···π and I···π interactions on the supramolecular arrangement. *Z. Anorg. Allg. Chem.* **2022**, *648*, e202200087. [CrossRef]
34. Morscher, A.; de Souza, M.V.N.; Wardell, J.L.; Harrison, W.T.A. Expected and unexpected products of reactions of 2-hydrazinylbenzo-thia-zole with 3-nitro-benzene-sulfonyl chloride in different solvents. *Acta Crystallogr. E Crystallogr. Commun.* **2018**, *74*, 673–677. [CrossRef]
35. *CrysAlisPro Software System*; Version 1.171.38.41; Rigaku Oxford Diffraction: The Woodlands, TX, USA, 2015.
36. McArdle, P.; Gilligan, K.; Cunningham, D.; Dark, R.; Mahon, M. OSCAIL: A method for the prediction of the crystal structure of ionic organic compounds—The crystal structures of o-toluidinium chloride and bromide and polymorphism of bicifadine hydrochloride. *CrystEngComm* **2004**, *6*, 303–309. [CrossRef]
37. Sheldrick, G.M. SHELXT-Integrated Space-Group and Crystal-Structure Determination. *Acta Crystallogr.* **2015**, *A7*, 3–8. [CrossRef] [PubMed]
38. Hübschle, C.B.; Sheldrick, G.M.; Dittrich, B. ShelXle: A Qt Graphical User Interface for SHELXL. *J. Appl. Crystallogr.* **2011**, *44*, 1281–1284. [CrossRef] [PubMed]

39. Sheldrick, G.M. *SHELXL-2018 (2018) Program for Crystal Structure Refinement*; University of Göttingen: Göttingen, Germany, 2018.
40. Spek, A.L. Structure validation in chemical crystallography. *Acta Crystallogr.* **2009**, *D65*, 148–155. [CrossRef] [PubMed]
41. Macrae, C.F.; Sovago, I.; Cottrell, S.J.; Galek, P.T.A.; McCabe, P.; Pidcock, E.; Platings, M.; Shields, G.P.; Stevens, J.S.; Towler, M.; et al. *Mercury 4.0*: From visualization to analysis, design and prediction. *J. Appl. Crystallogr.* **2020**, *53*, 226–235. [CrossRef] [PubMed]
42. Gavezzotti, A. Calculation of intermolecular interaction energies by direct numerical integration over electron densities. 2. An improved polarization model and the evaluation of dispersion and repulsion energies. *J. Phys. Chem.* **2003**, *B107*, 2344–2353. [CrossRef]
43. Gavezzotti, A. Calculation of lattice energies of organic crystals: The PIXEL integration method in comparison with more traditional methods. *Z. Für Krist. Cryst. Mater.* **2005**, *220*, 499–510. [CrossRef]
44. McKinnon, J.J.; Spackman, M.A.; Mitchell, A.S. Novel tools for visualizing and exploring intermolecular interactions in molecular crystals. *Acta Crystallogr.* **2004**, *B60*, 627–668. [CrossRef] [PubMed]
45. Wolff, S.K.; Grimwood, D.J.; McKinnon, J.J.; Turner, M.J.; Jayatilaka, D.; Spackman, M.A. *Crystal Explorer*; The University of Western Australia: Crawley, Australia, 2012.
46. Becke, A.D. Density-Functional Thermochemistry. III. The Role of Exact Exchange. *J. Chem. Phys.* **1993**, *98*, 5648–5652. [CrossRef]
47. Stephens, P.J.; Devlin, F.J.; Chabalowski, C.F.; Frisch, M.J. Ab Initio Calculation of Vibrational Absorption and Circular Dichroism Spectra Using Density Functional Force Fields. *J. Phys. Chem.* **1994**, *98*, 11623–11627. [CrossRef]
48. Azzam, R.A.; Elgemeie, G.H.; Elsayed, R.E.; Jones, P.G. Crystal structure of N′-[2-(benzo[d]thia-zol-2-yl)acet-yl]-4-methyl-benzene-sulfono-hydrazide. *Acta Crystallogr.* **2017**, *E73*, 1041–1043. [CrossRef]
49. Pai, N.; Foro, S.; Gowda, B.T. Crystal structure and Hirshfeld surface analysis of (*Z*)-4-chloro-*N*′-(4-oxo-thia-zol-idin-2-yl-idene)benzene-sulfono-hydrazide monohydrate. *Acta Crystallogr. Sect. E Crystallogr. Commun.* **2018**, *74*, 1569–1573. [CrossRef] [PubMed]
50. Song, Q.B.; Jin, Z.M.; Wang, H.B.; Jiang, B. N′-(Benzenesulfonyl)-4-methylthiazole-5-carbohydrazide. *Acta Crystallog.* **2004**, *E60*, o1292–o1293. [CrossRef]